



Shahrood University of  
Technology



Iranian Society of  
Mining Engineering  
(IRSM)

## Integration of Fractal and Multivariate Principal Component Models for Separating Pb-Zn Mineral Contaminated Areas

Hossein Mahdianfar<sup>1</sup> and Mirmahdi Seyedrahimi Niarag<sup>2\*</sup>

1. Department of Mining Engineering, University of Gonabad, Gonabad, Iran

2. Faculty of Engineering, University of Mohaghegh Ardabili, Ardabil, Iran

### Article Info

Received 6 June 2023

Received in Revised form 21 June 2023

Accepted 28 June 2023

Published online 28 June 2023

DOI: [10.22044/jme.2023.13227.2424](https://doi.org/10.22044/jme.2023.13227.2424)

### Keywords

Fractal model

Principal component analysis

Environmental pollution

Geo-chemical signals

### Abstract

The primary purpose of this investigation is contamination mapping in surrounding areas of Irankuh Pb-Zn mine, located in central Iran, using an integrated approach of principal component analysis (PCA) with the Concentration-Area (C-A) and Power Spectrum-Area (S-A) fractal models. PCA categorized the 45 elements into eight principal components. Component 2, containing the toxic elements of Pb, Zn, As, Mn, Cd, and Ba, was identified as the contamination factor. This multivariate contamination factor was modeled using the C-A and S-A fractal methods (in spatial and frequency domains) to delineate pollution areas. Modeling of PCA data using the C-A fractal method showed four main populations for the contamination factors. Two populations with higher fractal dimensions are associated with contamination from mining activities or anthropogenic effects. Low fractal dimensions are considered the background population, which has not been affected or is less affected by these activities. Five geo-chemical populations were obtained for contamination factors using the S-A fractal modeling of PCA in the frequency domain. Therefore, various geo-chemical populations were achieved using geo-chemical filtering and two-dimensional inverse Fourier transformation. The geo-chemical populations related to classes 2, 3, and 4 containing intermediate frequency signals showed the pollution anomaly. The spatial distribution of pollutant geo-chemical signals exhibits excellent conformity with the mining operation limit and tailing dam location as pollutant sources. The results indicate that the elements Pb, Zn, Cd, and As have significant values in the surrounding soils rather than their concentrations in the earth's crust. The results demonstrate that the S-A fractal models can more precisely delineate the environmental anomaly than the C-A fractal model, especially in intermediate frequency populations.

## 1. Introduction

Sustaining the soil and agricultural areas from the accumulation of toxic and heavy metals holds a fundamental role in food security, human health, and animals' survival [1]. Soils are polluted by toxic metals from the sources of natural and human. Mineral mining, as a human factor, can effectively transfer heavy and toxic metals to the environment [2, 3]. Sources detecting and spatial distribution mapping toxic elements in the soil are essential for pollution control [4]. Identifying the features of the metal pollution process and delineating the polluted areas are fundamental tasks to prevent pollution [5]. The anomaly

mapping methods performed in the mineral geochemical exploration can be utilized desirably for contamination mapping in environmental geochemistry [6].

Various univariate and multivariate methods such as fractal models [7-12], probability plots [13-15], PCA [16, 17] and machine learning algorithms [1, 18] have been applied for anomaly mapping in mineral geo-chemical exploration. The univariate methods of probability plot and fractal models have been performed for environmental geochemical anomaly mapping [19]. Multivariate methods such as principal component analysis have been

✉ Corresponding author: [M.seydrhimi@uma.ac.ir](mailto:M.seydrhimi@uma.ac.ir) (M.M. Seyedrahimi Niarag)

effectively applied for spatial distribution mapping of toxic metals [4, 20, 21].

Multivariate signatures in mining and environmental geo-chemistry are not considered by applying simple fractal models. PCA has been applied for discerning geochemical patterns in the spatial, frequency, and wavelet domains in mining geo-chemistry [22-29]. PCA can be used to reduce the dimensions of the environmental dataset and identify the heavy and toxic elements related to the pollution process. This multivariate method has been applied for environmental geochemical mapping and contamination source detecting relevant to mining works [20]. PCA can identify the essential influence variables in the pollution process concealed in environmental geochemical datasets based on correlations and internal relations of elements [30, 31]. This method extracts desirable information from complicated geo-chemical datasets [32]. The new multivariate features with new scores are calculated for each sample in the rotated space that can be analyzed as independent integrated factors. The principal factor of toxic elements can be modeled and mapped using various methods such as C-A and S-A fractal approaches. The C-A fractal method has been developed to detect exploration geochemical anomalies [7, 15, 33, 34] and has been used to map contaminated areas of univariate elements [35, 36]. S-A fractal method is used to identify frequency features relevant to geo-chemical populations concealed in the dataset [37, 38]. The geo-chemical frequency signals of elements have been frequently modeled using a fractal method in mining geo-chemistry [8, 38, 39].

In this study, new integrated techniques were applied based on the principal component scores and C-A and S-A fractal models in the spatial and frequency domains for the first time to characterize pollution phenomena in the surrounding soils of mining activities. The PC of the pollution process has been modeled by fractal techniques in the spatial and frequency domains. Therefore, the fractal populations of geo-chemical signals as multi-element environmental pollution factors have been distinguished. These methods can identify the variables related to contamination and separate the areas affected by toxic metal pollution with more certainty.

## 2. Case Study

Irankuh mine is located in the vicinity of Irankuh mountain in the Isfahan province, Iran. This area is part of the Sanandaj-Sirjan zone. This zone is a unit of the Zagros orogen, which includes metamorphic rocks [6, 40, 41]. The geological map of the study area, on which soil geochemical samples and main land uses are fitted, is shown in Figure 1. This area hosts Zn-Pb deposits related to Malayer-Isfahan metallogenic belt. A cretaceous sequence of dolostone and fossiliferous calcareous rocks overlay a Jurassic shale layer, which is the lowest stratigraphic unit in the area [42, 43]. Sulfides and carbonates include the MVT Pb-Zn mineralization that occurred in dolostones. Open-pit and underground mining has been carried out in this area for several decades. Mineral processing plants, tailings, and waste piles are located near the agricultural areas in the southern part of Irankuh.

In the Irankuh region, epigenetic Pb-Zn mineralization, covered by lower Cretaceous dolostone and Jurassic shale, has occurred. This mineralization was formed within the dolomite and shale host rocks by a series of replacement processes and appeared in the forms of veinlets, breccia, and filled spaces [44]. The primary lead-zinc mineralization is in the form of altered hydrothermal veins in fractured rocks, reverse faults, and dilatational spaces. These alterations include dolomitization and silicification. It can be concluded that this mineralization occurred during or after fracturing and faulting [45]. The iron and manganese-rich dolomite, iron-rich sphalerite, ankerite, low pyrite, galena, bituminous, calcite  $\pm$  quartz  $\pm$  barite are the dominant minerals of this mineralization [44].

The climate of the study area is semi-arid, and it is usually windy from March to May and sometimes from September to October [45]. The pH of the regional soil is around 7-8, and its chemical composition is organic compounds, calcic, and some salt. Regarding soil size, the approximate percentages of sand, silt, and clay are 44, 39, and 17, respectively [35]. Near the mine, plants and agricultural products are contaminated with toxic metals such as lead and zinc. These metals are dispersed in the region through the dust. Therefore, it has created concerns for the region's farmers [46].

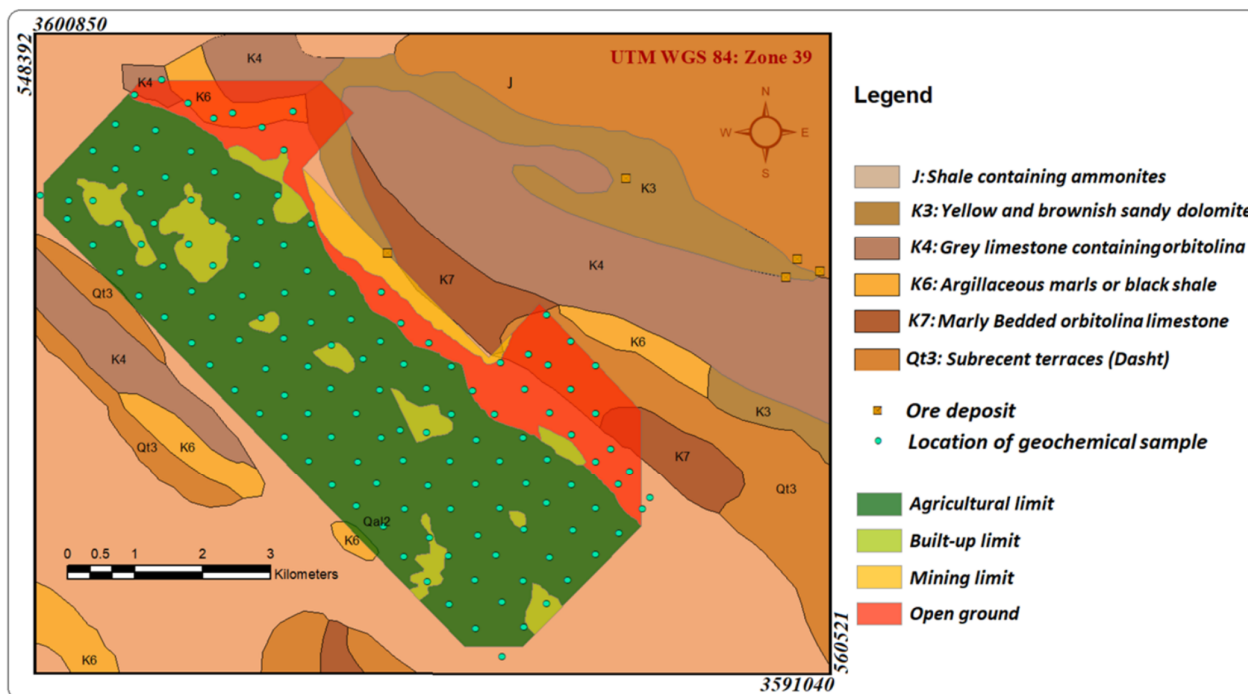


Figure 1. Geological map of the Irankuh region; location of the soil samples and primary land use is shown on the map.

### 3. Materials and Methods

#### 3.1. Dataset

One hundred thirty-seven soil geochemical samples were taken from the depth of 0 to 30 cm around the mining areas. These areas include the spanning small industrial/residential and larger agricultural areas. To collect these samples, a grid of 500 × 500 square meters was designed (Figure 1). Considering the situation of the field, the location of some sampling sites has been adjusted. The samples were prepared with a four-acid mix (HCl–HNO<sub>3</sub>–HClO<sub>4</sub>–HF) and analyzed for 44 elements. These samples have been analyzed by inductively coupled plasma-optical emission spectrometry in the central laboratory of the Geological Survey and Mineral Exploration of Iran with a detection limit of elements of 0.1. Figure 2 shows the carbonate layer located south of the Irankuh limit, next to which is the farmers' greenhouses. Also in this figure, close to the location, the tailing dam located in the southern part of the area is clearly shown.



Figure 2. Photo of the carbonate unit, greenhouses, and tailing dam in the southern part of Irankuh limit (looking north).

**3.2. C-A fractal modeling of PCA**

PCA is a typical multivariate analysis and dimension reduction technique. It extracts new uncorrelated components from several correlated features and reduces the dimensionality of feature space in the dataset [32]. PCA is performed on a dataset based on the calculated covariance or correlations of features. The principal components as coordinate axes in the new features space have been achieved using the Varimax rotation method. The Varimax method reveals the complicated structures of datasets [47, 48]. This orthogonal rotation method can simplify structures by transforming the component subspace of PCA. The Varimax function maximizes the sums of squares of the loadings for original variables. The interpretation of the dataset can be improved by rotating the matrix of principal components coefficients [47, 49].

New values for each sample are calculated based on the rotated axes in the new space. Therefore, each sample holds an absolute principal component score related to any principal component. These scores as new multivariate geochemical features can be analyzed instead of concentrations of elements. The scores of samples related to pollution factors are computed using the below equation:

$$Score_{(Pollution\ Factor)} = b_1X_1 + b_2X_2 + \dots + b_pX_p \quad (1)$$

where coefficients of b are related to the regression weight of principal components calculated during the PCA procedure, and X values are the initial concentration of elements that contribute to making the pollution factor. The PCs extracted by PCA can be modeled using fractal methods. Determining the fractal dimension is the basis of the fractal method for determining geochemical patterns. A smooth model of the spatial distribution of elements is provided by contour maps. If, in these maps,  $A(\rho)$  is an area of a contour with a concentration of  $\rho$ , then the area decreases with increasing concentration. To define

the background and geochemical anomaly, the concentration-area fractal model is defined as follows [7]:

$$A(\rho)_{(>\rho)} \propto \rho^{-D} \quad (2)$$

where  $A(\rho)$  is the contour area with a concentration more significant than the value of  $\rho$ , and D is exponential features or fractal dimensions.

A grid of cells can be overlapped over the study area. In this case,  $A(\rho)$  can be obtained by counting cells with a raw concentration of elements. In this method, for concentrations higher than the desired counter,  $A(\rho)$  is equal to the number of cells multiplied by the area of the cells. Considering that in geo-chemical surveys, anomalies show concentrations related to mineralization processes, these values will have power functions or fractal dimensions different from background values. This difference in fractal dimensions is used to separate anomalous areas from the background [7, 34, 36, 50]. Geochemical anomalies have larger fractal dimensions than the populations of the geochemical background. Therefore, the border between these fractal dimensions can be considered threshold values. The threshold value separates anomalous values from the geochemical background. The C-A fractal modeling of PCA categorizes the contamination populations and intensifies the environmental geochemical anomaly.

**3.3. S-A fractal modeling of PCA**

PCA can extract new principal factors using the Varimax rotation method. The pollution factor containing the mentioned scores for each sample can be interpreted as a new geochemical index. Spectral analysis of this pollution index in the frequency domain is a mathematical approach for pollution mapping. Hence, the pollution factor can be converted to the frequency domain using two dimensional Fourier transformation function as follows [51]:

---


$$F(K_x, K_y) = \int_{-\infty}^{\infty} \int_{-\infty}^{\infty} f(x, y) \cos(K_x x + K_y y) dx dy - i \int_{-\infty}^{\infty} \int_{-\infty}^{\infty} f(x, y) \sin(K_x x + K_y y) dx dy \quad (3)$$


---

where  $f(x, y)$  is the pollution factor as a spatial function, and  $K_x$  and  $K_y$  indicate the wave number values in the x and y directions.  $F(K_x, K_y)$  containing the real part,  $R(K_x, K_y)$ , and imaginary part,  $I(K_x, K_y)$ , is a transferred function in the

frequency domain. The power spectrum values are calculated as follows [51]:

$$E(K_x, K_y) = R^2(K_x, K_y) + I^2(K_x, K_y) \quad (4)$$

The log-log plot of fractal based on the power spectrum and cumulative areas are delineated, and different straight lines are fitted on points of the log-log graph. The threshold values for geo-chemical classes are detected using the breakdown points of the graph and show the various power-law relationships. The S-A fractal models are defined as follows:

$$A(\geq S)\alpha S^{-2d/\beta} \quad (5)$$

where  $A(>S)$  indicates the areas larger and equal to power spectrum value ( $S$ ), and  $\beta$  is the amount of anisotropy, and  $d$  is the generalized scale invariance parameter. The geo-chemical classes are separated using low, high, and band pass filtering, and then are transferred to the spatial domain using inverse Fourier transformation. These separated classes can illustrate the various geochemical populations consisting of geochemical noise, background, and anomaly.

#### 4. Results

The agricultural, industrial, and residential backgrounds, which include surrounding areas of the Pb-Zn mine, have been affected by pollution from mining activities. In this research work, the data obtained from the analysis of 137 soil samples were collected. The histogram and some statistical parameters of Pb, Zn, Cd, As, and Ba are presented in Figure 3. The average concentration of these elements in the earth's crust are 12.5, 70, 0.2, 1.8, and 425 ppm, respectively [52]. Figure 3 shows that the histograms of lead, zinc, cadmium, and arsenic follow an abnormal distribution, and barium has a normal distribution. The highest frequency is around the average concentration of these elements in the study area. This amount is several times the Clark of the elements. The results obtained from geo-chemical surveys and patterns of contaminant elements and the relationship between these elements show that the leading cause of environmental pollution of surrounding areas with toxic metals is dust [35, 40].

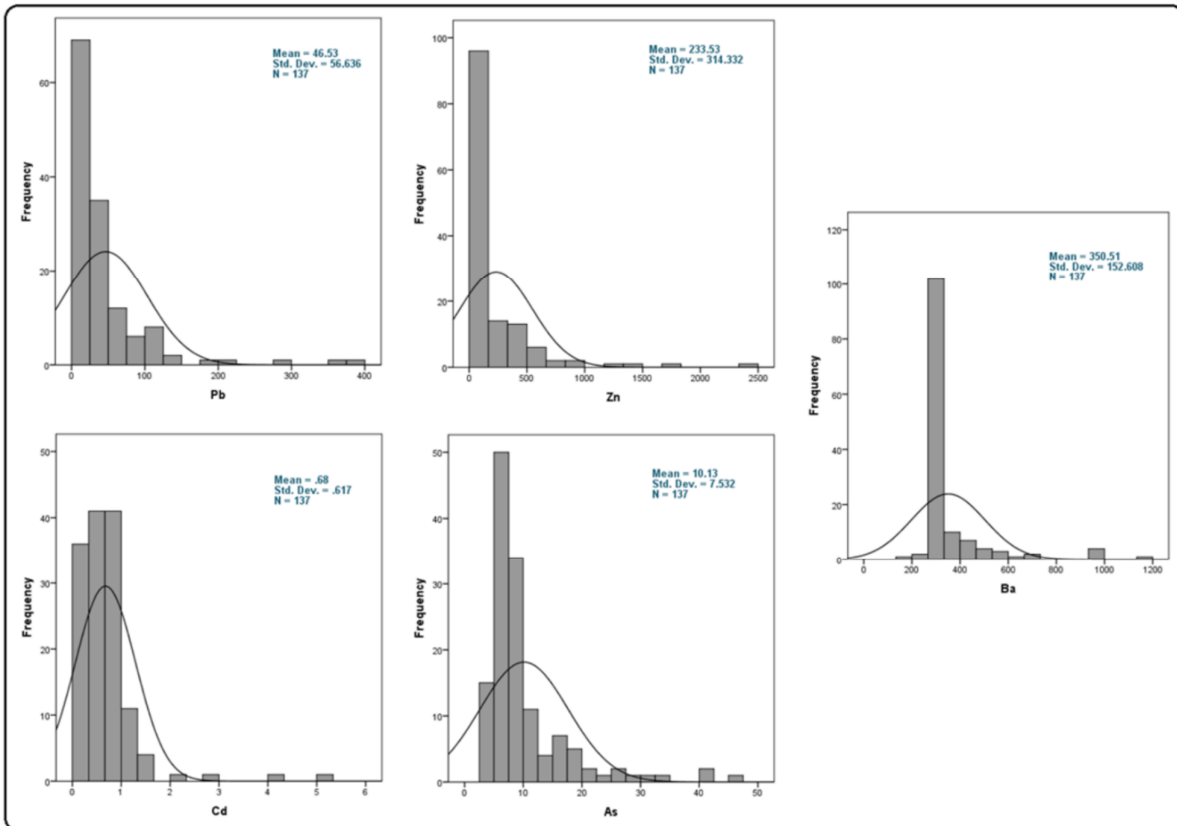


Figure 3. Histogram of the toxic elements along with some statistical parameters in the studied area.

The ratio of the average and maximum concentration of samples in the studied area to the average concentration of the toxic elements in the

earth's crust [52] has been delineated in Figure 4. These values demonstrate that mining activities polluted the surrounding areas of the Irankooch Pb-

Zn mine with toxic elements, especially Cd, Pb, Zn, and As. In this investigation, the contaminated surrounding areas were mapped using the C-A and

S-A fractal modeling of multivariate pollution factors obtained by PCA.

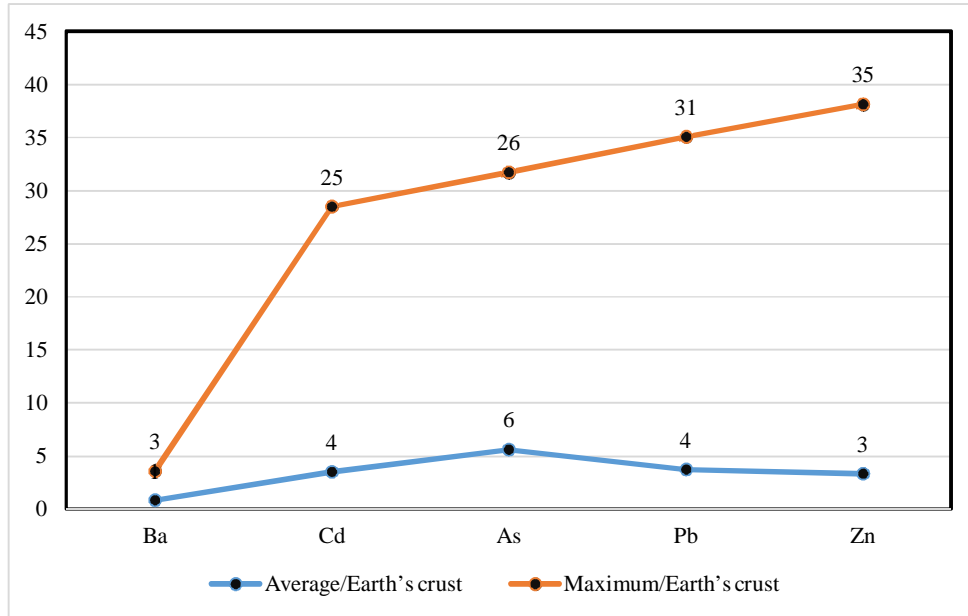


**Figure 4.** Ratio of the average and maximum concentration of samples in the studied area to the average concentration of the toxic elements in the earth's crust.

#### 4.1. PCA method

The surrounding areas of the Irankooh Pb-Zn mine have been contaminated by toxic elements especially lead and zinc. In this study, the multivariate pollution factor consisting of toxic elements was investigated. The concentrations of 45 elements were applied for detecting the pollution factor using PCA based on the correlation matrix of elements. The log-ratio geo-chemical data were analyzed using PCA. The integrated environmental anomaly caused by toxic elements can be obtained by PCA. The relevance of toxic metals in the soil samples was quantified using PCA as a feature extraction method. The correlation matrix, Varimax rotation, and Kaiser normalization methods were performed for extracting the PCs.

The Kaiser normalization method was applied to the dataset. Then the geochemical data were rotated in the new coordinate system using the Varimax rotation method. The PCs as new features are obtained based on the new rotated axes. The 45 elements were categorized in 8 PCs with a cumulative variance of 86% for initial eigenvalues using PCA. The variances of these deriving PCs are shown in Figure 5. Figure 6 shows the component loadings of elements in the second PC. The elements of Pb, Zn, As, Ba, Cd, and Mn have component loadings of more than 0.5 and significantly affect this component as a pollution factor. These toxic elements have also been separated from other elements in the plot of PCs of 1, 2, and 3 in rotated space (Figure 7). The PC scores of deriving pollution factors that indicate the contamination magnitude of soil are calculated for all samples using PCA equations.

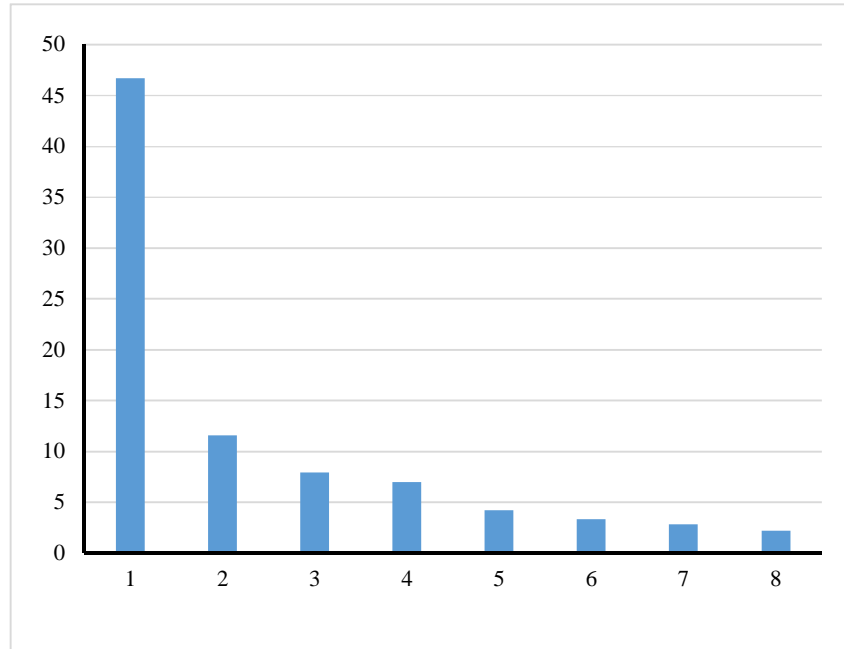


Figure 5. Variances of the deriving PCs from PCA.

4.2. C-A fractal modeling of PCA

In order to C-A fractal modeling of PCA, the fractal model for the positive values is drawn, modeled, and calculated as the threshold value for the anomalous sub-population. To model the PCA scores by fractal method, the negative PCA values must convert to a positive value. For this aim, the PCA scores can be shifted by adding a constant positive number. The spatial location of the

anomaly samples and mineralized zones are not changed using this transformation. Modeling the negative scores of the PCA in order to determine the threshold values is one of the development of the article. Firstly, the usual PCA method was done on the log-ratio geochemical data to prepare the input for modeling. In the next step, to generate positive data, a fixed number was added to all pollution factor scores. Then new PCA scores were used and modeled by the C-A fractal method.

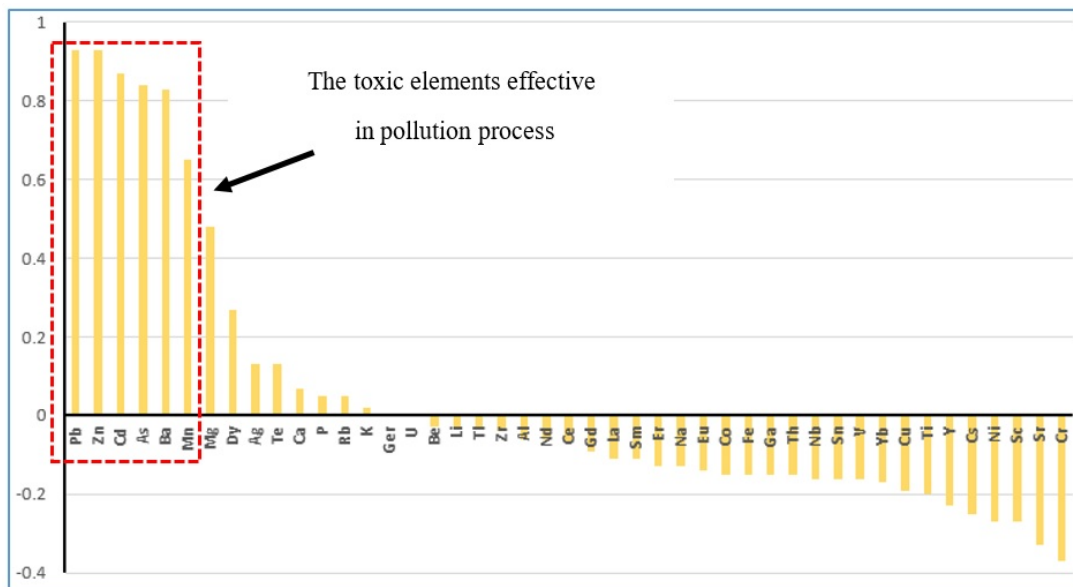


Figure 6. Component loading of elements in the pollution factor obtained by PCA and the practical toxic elements.

A grid net of  $91 \times 91 \text{ m}^2$  (with a total number of 9498 grids) was used to estimate the concentration and interpolate the data using the ordinary kriging technique. The mentioned interpolation technique was implemented on the PCA scores. After the estimation stage of the network and classification of the estimated data, the logarithmic plot of the concentration-area was drawn on the variables. On this graph, different populations with different fractal dimensions were recognized (Figure 8). There are four main populations on the C-A fractal

diagram for multivariate pollution factors. Fractal dimensions generally increase from low to high concentration populations. The anthropological effects of mining activities or anomalous populations were recognized with high fractal dimensions. Low fractal dimensions are also related to the background populations that have not been affected or are less affected by these activities [7, 34, 53, 54]. Fractal dimensions obtained from primary populations identified four populations 1 to 4 are 0.06, 2.14, 0.75, and 7.35, respectively.

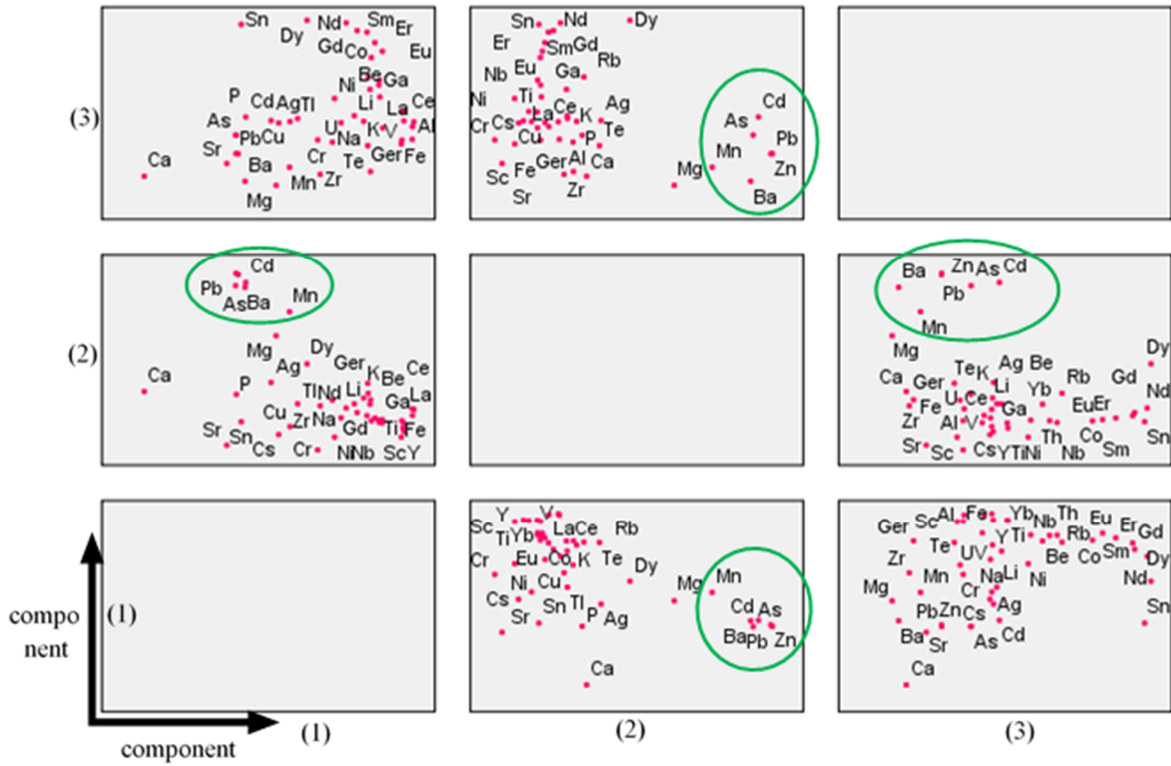


Figure 7. Component plot of principal components 1, 2, and 3 in rotated space, the toxic elements related to pollution phenomena have been detected.

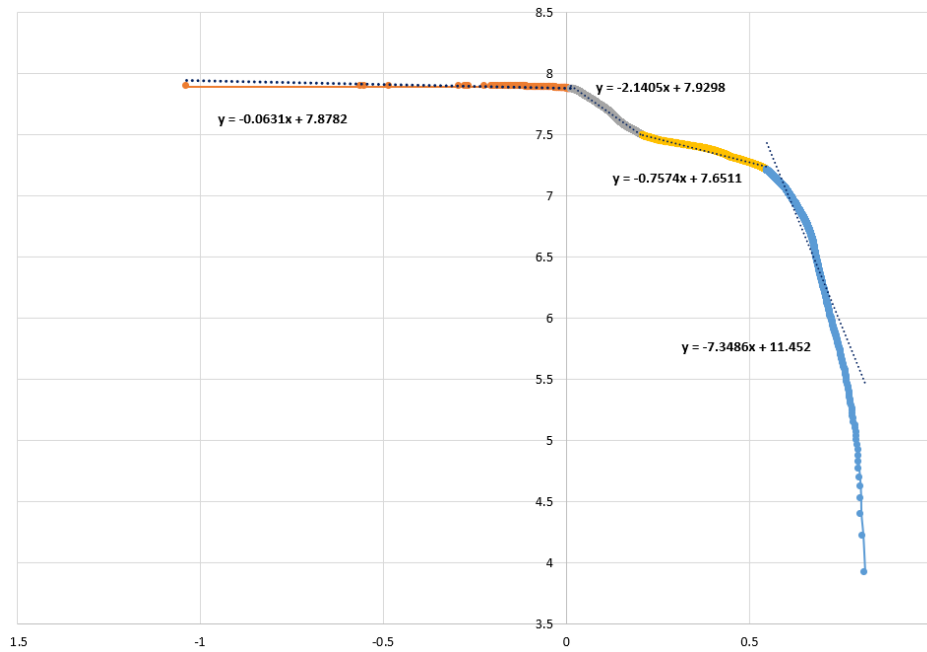


Figure 8. C–A fractal model of PC2 data.

**4.3. S-A fractal modeling of PCA**

The multivariate geochemical map can be created using S-A fractal modeling of PCA [36]. In this study, PCA was applied to identify the pollution factor. The pollution factor (PC2), integrated from the toxic elements of Pb, Zn, As, Ba, Cd, and Mn, improves the multi-element geochemical signature. This integrated factor was modeled using the S-A fractal method. For this

aim, the pollution factor was transformed to the frequency domain, and the power spectrum values relevant to the contamination signals were calculated using the two-dimensional fast Fourier function. The power spectrum distribution map of the pollution factor is depicted in Figure 9. This map indicates the wavenumbers and the power values of the constituent signals of the pollution factor.

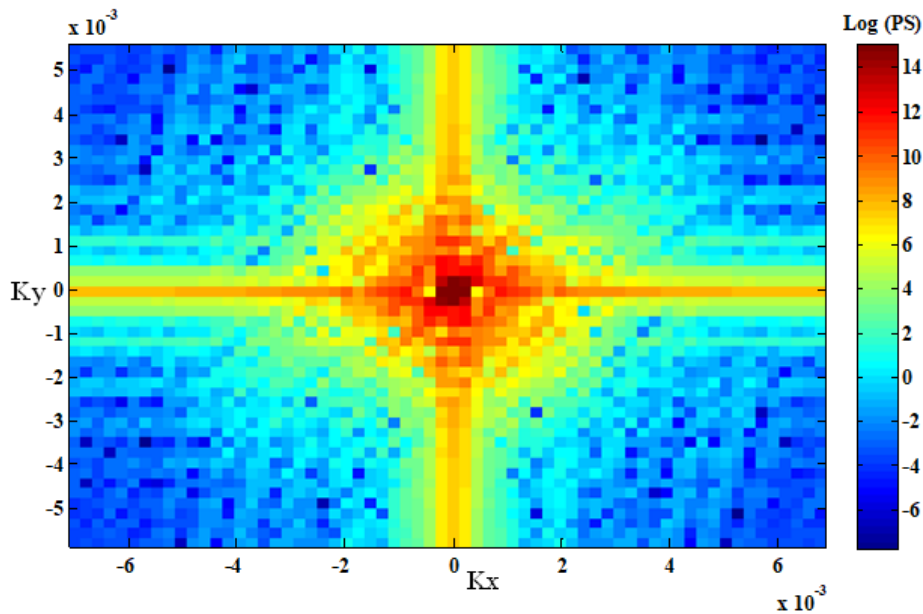


Figure 9. Distribution map of logarithmic power spectrum values related to the multivariate integrated pollution factor (containing As, Pb, Zn, Cd, Ba, Mn elements).

The distribution map of the power spectrum related to the integrated pollution factor was applied for delineating the logarithmic S-A fractal plot (Figure 10). The logarithmic values of the power spectrum (PS) versus area were plotted in this modeling. Based on the least squares method,

five straight lines were fitted to these data points, and five geochemical classes were detected with various power-law relationships. The features of these frequency classes extracted from fractal modeling have been represented in Table 1.

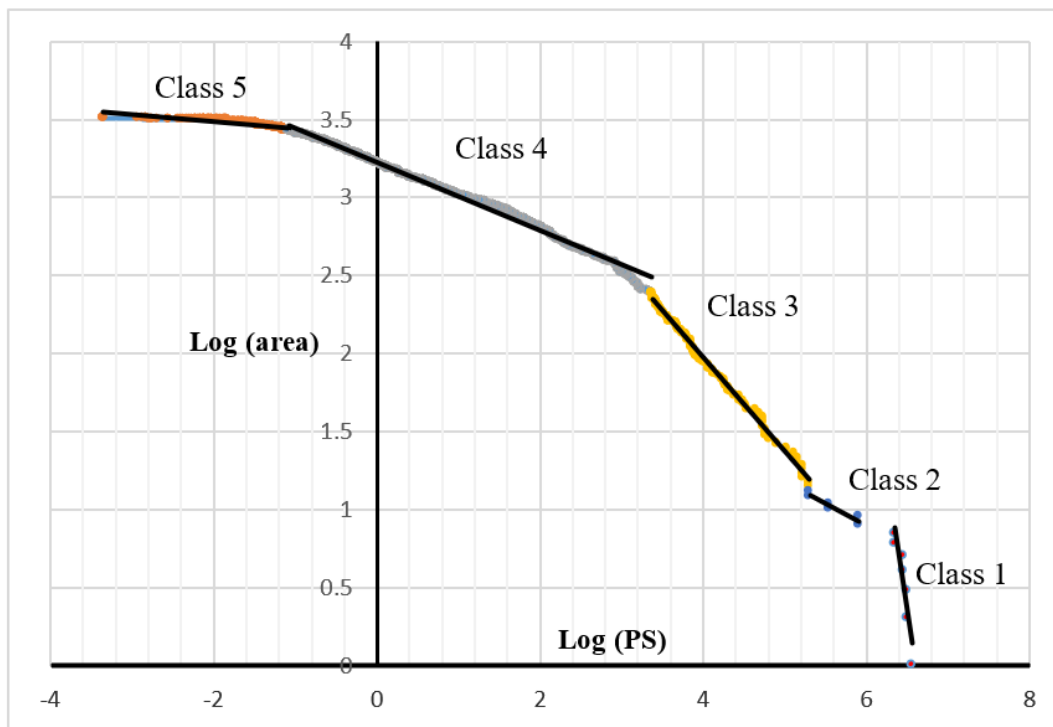


Figure 10. S-A fractal plot of the power energy, Log (PS), versus cumulative area, Log (area), related to the multivariate pollution factor of PCA.

Table 1. Characteristics of 5 geo-chemical classes obtained from the S-A fractal model of pollution factor.

Geo-chemical class	Class 1	Class 2	Class 3	Class 4	Class 5
Thresholds (PS)	2271082-3713604	206298-2271082	2403- 206298	0.083 - 2403	0.00044 – 0.083
Frequency signals	Very low	Low	Moderate	High	Very high
Fractal dimension	3.46	0.3	0.6	0.21	0.04

**5. Discussion**

Figure 11 shows a multivariate geo-chemical map. This map is obtained from the fractal concentration-area modeling of PCA data. In this integrated method, contour maps with pixels of acceptable size were provided using a kriging interpolation technique on PCA scores. Based on variables Pb, Zn, As, Ba, Mn, and Cd, four multi-element different populations are separated on this

map. Higher populations are shown with magenta and purple colors, the intermediate population with dark turquoise color, and the background population with turquoise color. Higher concentrations of elements are included in the mining limit and its surroundings. The open-ground limit is related to concentrations with an intermediate population (Figure 1). The center and southwest of the area are also related to the background population.

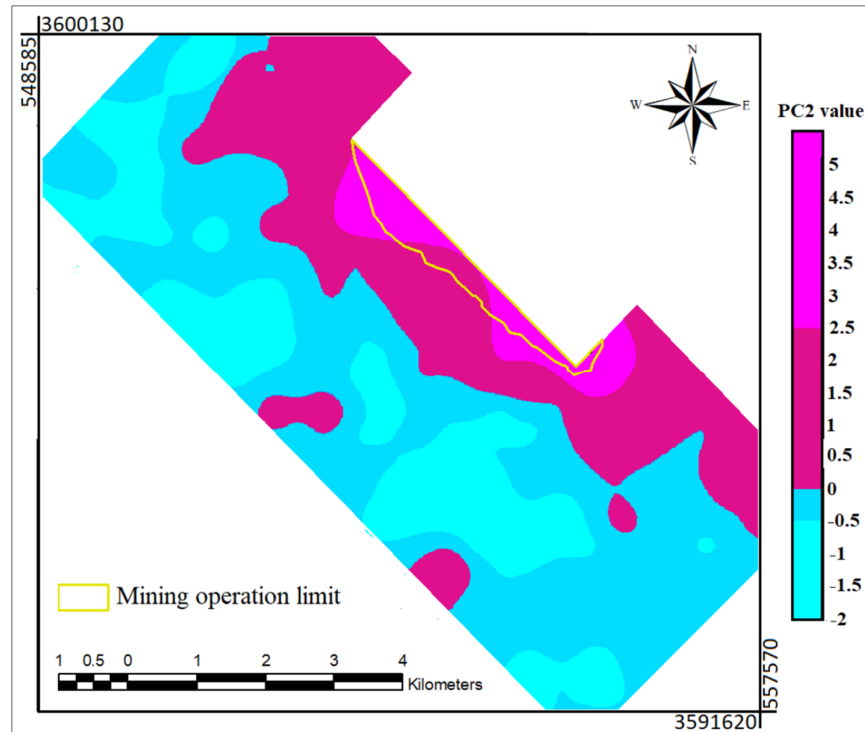


**Figure 11. Geochemical pollution map resulted from C-A fractal modeling of PC2 with four populations in the studied area.**

Different PS-based filter functions were designed to separate the geochemical classes detected by the fractal plot. The PS-based filter functions only filter some PS values and ignore the frequencies and wavelength values [24, 55].

The right-hand line in the fractal plot containing very low-frequency signals is relevant to background values. The left-hand population represents the very high-frequency signals commonly considered noise factor in geochemical data. The geochemical noises can be related to inaccuracy and imprecision of sampling, preparation, and analyzing steps. The intermediate frequency signals commonly indicate anomaly

signatures in the frequency domain. In this investigation, five geochemical contamination classes were identified using fractal modeling of the integrated pollution factor of PCA. Five PS-based filter functions were designed and applied to separate the five fractal classes (Table 2). These filters have been defined using the obtained threshold values of the fractal diagram. The inverse Fourier transform was applied for transforming the five frequency classes to the spatial domain. The geochemical populations of background, noise, and anomaly classes are effectively identified using the S-A fractal model.

**Table 2. Five geo-chemical classes obtained from the S-A fractal model of pollution factor and their applied filter functions.**

Geo-chemical population	Applied filter function
Class 1	$G(Kx, Ky) = \begin{cases} 1 & 2271082 \leq PS \\ 0 & 2271082 > PS \end{cases}$
Class 2	$G(Kx, Ky) = \begin{cases} 1 & 206298 < PS \leq 271082 \\ 0 & \text{otherwise} \end{cases}$
Class 3	$G(Kx, Ky) = \begin{cases} 1 & 2403 < PS \leq 206298 \\ 0 & \text{otherwise} \end{cases}$
Class 4	$G(Kx, Ky) = \begin{cases} 1 & 0.083 < PS \leq 2403 \\ 0 & \text{otherwise} \end{cases}$
Class 5	$G(Kx, Ky) = \begin{cases} 1 & PS \leq 0.083 \\ 0 & \text{otherwise} \end{cases}$

The frequency signals in fractal class 1 were separated and transformed into the spatial domain using 2DFT. The very low-frequency signals are relevant to the background values, and Figure 12a indicates the distribution map of these fractal classes. The pollution areas and the origin of contamination are not detected using this frequency class. Figure 12b indicates the geochemical distribution map of low-frequency signals in the spatial domain. The fractal class 3, including the moderated signals, properly deposes the pollution process (Figure 12c). The geochemical anomaly and origin of contamination have been detected by interpreting this class. Pollution anomalies consisting of moderate frequency signals between the PS of 2403 and 271082 occur around the mining activities. Significant pollution anomalies related to PS values between 0.083 and 2403 based on the S-A fractal model (class 4) are situated near the tailing dam and the location of mining activities (Figure 12d).

The fractal class 5, consisting of very high-frequency signals, is relevant to the geochemical noises. The geo-chemical distribution map of these very high-frequency signals is shown in Figure 12e. These high-frequency signals create shallow

scores for pollution factors in the spatial domain. This map indicates that the low part of the multi-element pollution factor is related to geo-chemical noises.

The fractal classes 2, 3, and 4 containing frequency signals related to geochemical anomalies were combined to indicate a proper prospectively map. Hence, the signals of classes 1 and 5 were filtered and removed from data using newly designed filter function that preserves the PS values between 0.083 and 271082. The residual signals were transformed to the spatial domain using 2DIFT for mapping the pollution geochemical anomalies (Figure 12f). These integrated fractal classes have yielded a proper correlation between anomalies and pollution sources and distinguish essential targets for future contamination studies. The obtained integrated environmental anomalies are closely related to mining activities. The integration of PCA and the S-A fractal method is a practical scenario for detecting the sources of toxic metal pollution and recognizing the polluted areas. The S-A fractal method that categorizes the various geochemical frequency signals could more precisely indicate the contaminated environmental areas rather than the C-A fractal method.

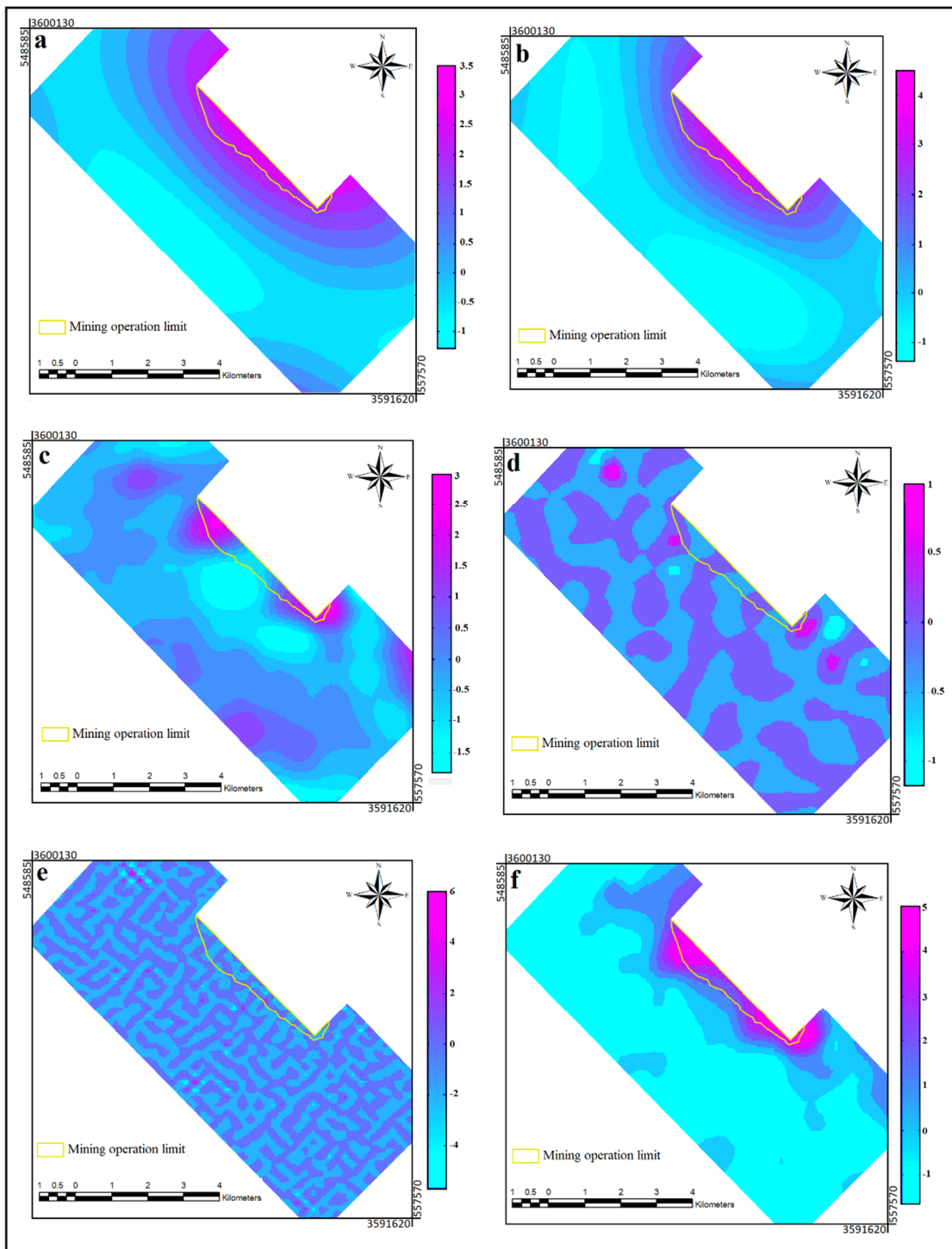


**Figure 12. Geo-chemical contamination map of the frequency classes compiled using the S-A fractal model, a: frequency class 1, b: frequency class 2, c: frequency class 3, d: frequency class 4, e: frequency class 5, f: combined frequency classes 2, 3, and 4.**

**6. Conclusions**

New integrated techniques were developed based on modeling of the PCA method results by the C-A and S-A fractal models for identifying pollution

areas in the surrounding soils of mining activities. The main findings of this study are as follows:

1. The PCA method extracted 8 PCs, including a cumulative variance of 86% from 45 elements using the varimax analytic rotation.

2. The C-A fractal model shows four main geochemical populations for multivariate pollution factors. High fractal dimensions are associated with contamination from mining activities. The fractal dimension of primary populations recognized four populations.
3. A multivariate geochemical map obtained from modeling PCA data by the C-A fractal method determined the concentration of elements in the mining limit. Also, it revealed the concentration of toxic elements in the open-ground limit.
4. The S-A fractal model indicated five geochemical populations for multivariate pollution factors. The surrounding areas of Irankooch have mainly been polluted by toxic elements that are closely relevant to mining activities.
5. The pollution anomalies detected by C-A and S-A fractal modeling of PCA coincide closely with contamination areas and are correlated to pollution sources. The obtained results demonstrate that the fractal populations of the S-A method can more precisely detect the pollution areas rather than the C-A fractal model.

### Acknowledgments

The authors appreciate the Iranian Geological Survey for analyzing the soil samples and supporting the project.

### References

- [1]. Zhang, B., Jia, T., Peng, S., Yu, X., and She, D. (2022). Spatial distribution, source identification, and risk assessment of heavy metals in the cultivated soil of the Qinghai-Tibet Plateau region: Case study on Huzhu County. *Global Ecology and Conservation*, e02073.
- [2]. Diatta, J.B., Chudzinska, E., and Wirth, S. (2008). Assessment of heavy metal contamination of soils impacted by a zinc smelter activity. *Journal of Elementology*, 13 (1).
- [3]. Yousefi, M. and Hronsky, J.M. (2023). Translation of the function of hydrothermal mineralization-related focused fluid flux into a mappable exploration criterion for mineral exploration targeting. *Applied Geochemistry*, 105561.
- [4]. Anaman, R., Peng, C., Jiang, Z., Liu, X., Zhou, Z., Guo, Z., and Xiao, X. (2022). Identifying sources and transport routes of heavy metals in soil with different land uses around a smelting site by GIS based PCA and PMF. *Science of The Total Environment*, 153759.
- [5]. Huang, Y., Li, T., Wu, C., He, Z., Japenga, J., Deng, M., and Yang, X. (2015). An integrated approach to assess heavy metal source apportionment in peri-urban agricultural soils. *Journal of Hazardous materials*, 299, 540-549.
- [6]. Seyedrahimi-Niaraq, M., Mahdiyanfar, H., and Mokhtari, A.R. (2022). Integrating principal component analysis and U-statistics for mapping polluted areas in mining districts. *Journal of Geochemical Exploration*, 234, p.106924.
- [7]. Cheng, Q., Agterberg, F.P., and Ballantyne, S.B. (1994). The separation of geochemical anomalies from background by fractal methods. *Journal of Geochemical Exploration*, 51, 109-130.
- [8]. Zuo, R. (2014). Identification of geochemical anomalies associated with mineralization in the Fanshan district, Fujian, China. *Journal of Geochemical Exploration*, 139, 170-176.
- [9]. Rahimi, H., Abedi, M., Yousefi, M., Bahroudi, A., and Elyasi, G.R. (2021). Supervised mineral exploration targeting and the challenges with the selection of deposit and non-deposit sites thereof. *Applied Geochemistry*, 128, 104940.
- [10]. Afzal, P., Farhadi, S., Boveiri Konari, M., Shamseddin Meigooni, M., and Daneshvar Saein, L. (2022). Geochemical anomaly detection in the Irankuh District using Hybrid Machine learning technique and fractal modeling. *Geopersia*.
- [11]. Daneshvar Saein, L., Afzal, P., Shahbazi, S., and Sadeghi, B. (2022). Application of an improved zonality index model integrated with multivariate fractal analysis: epithermal gold deposits. *Geopersia*, 12 (2): 379-394.
- [12]. Paravarzar, S., Mokhtari, Z., Afzal, P., and Aliyari, F. (2023). Application of an approximate geostatistical simulation algorithm to delineate the gold mineralized zones characterized by fractal methodology. *Journal of African Earth Sciences*, 200, 104865.
- [13]. Sinclair, A.J. (1991). A fundamental approach to threshold estimation in exploration geochemistry: probability plots revisited. *Journal of Geochemical Exploration*, 41(1-2): pp.1-22.
- [14]. Moradpouri, F. and Ghavami-Riabi, R. (2020). A multivariate geochemical investigation of borehole samples for gold deposits exploration. *Geochemistry International*, 58, 40-48.
- [15]. Seyedrahimi-Niaraq, M. and Hekmatnejad, A. (2021). The efficiency and accuracy of probability diagram, spatial statistic and fractal methods in the identification of shear zone gold mineralization: a case study of the Saqqez gold ore district, NW Iran. *Acta Geochimica*.
- [16]. Xiao F, Wang K, Hou W, and Erten O. (2020). Identifying geochemical anomaly through spatially anisotropic singularity mapping: A case study from silver-gold deposit in Pangxidong district, SE China. *Journal of Geochemical Exploration*, 1; 210:106453.
- [17]. Farzamian, M., Mahdiyanfar, H., and Rouhani, A.K. (2022). Evidential belief functions modeling of geophysical and multi-element geochemical data for Pb-

Zn mineral potential targeting. *Journal of African Earth Sciences*, p.104606.

[18]. Farhadi, S., Afzal, P., Boveiri Konari, M., Daneshvar Saein, L., and Sadeghi, B. (2022). Combination of Machine Learning Algorithms with Concentration-Area Fractal Method for Soil Geochemical Anomaly Detection in Sediment-Hosted Irankuh Pb-Zn Deposit, Central Iran. *Minerals*. 12 (6): 689.

[19]. Borojerdnia A, Rozbahani M.M, Nazarpour A, Ghanavati N, and Payandeh K. (2020). Application of exploratory and Spatial Data Analysis (SDA), singularity matrix analysis, and fractal models to delineate background of potentially toxic elements: A case study of Ahvaz, SW Iran. *Science of the Total Environment*.10:140103.

[20]. Yang, Y., Yang, X., He, M., and Christakos, G. (2020). Beyond mere pollution source identification: Determination of land covers emitting soil heavy metals by combining PCA/APCS, GeoDetector and GIS analysis. *Catena*, 185, 104297.

[21]. Koohzadi, F., Afzal, P., Jahani, D., and Pourkermani, M. (2021). Geochemical exploration for Li in regional scale utilizing Staged Factor Analysis (SFA) and Spectrum-Area (SA) fractal model in north central Iran. *Iranian Journal of Earth Sciences*. 13 (4): 299-307.

[22]. Yousefi, M., Kamkar-Rouhani, A., and Carranza, E.J.M. (2012). Geochemical mineralization probability index (GMPI): a new approach to generate enhanced stream sediment geochemical evidential map for increasing probability of success in mineral potential mapping. *Journal of Geochemical Exploration*, 115, 24-35.

[23]. Shahi, H., Ghavami, R., Rouhani, A.K., Kahoo, A.R., and Haroni, H.A. (2015). Application of Fourier and wavelet approaches for identification of geochemical anomalies. *Journal of African Earth Sciences*, 106, 118-128.

[24]. Shahi, H., Ghavami, R., and Rouhani, A.K. (2016). Comparison of mineralization pattern of geochemical data in spatial and position-scale domain using new DWT-PCA approach. *Journal of the Geological Society of India*. 88 (2): 235-244.

[25]. Farzadian, M., Rouhani, A.K., Yarmohammadi, A., Shahi, H., Sabokbar, H.F., and Ziaie, M. (2016). A weighted fuzzy aggregation GIS model in the integration of geophysical data with geochemical and geological data for Pb-Zn exploration in Takab area, NW Iran. *Arabian Journal of Geosciences*. 9 (2): p.104.

[26]. Abedi, M., Kashani, S.B.M., Norouzi, G.H., and Yousefi, M. (2017). A deposit scale mineral prospectivity analysis: A comparison of various knowledge-driven approaches for porphyry copper targeting in Seridune, Iran. *Journal of African Earth Sciences*, 128, 127-146.

[27]. Mahdiyfar, H. (2020). Prediction of economic potential of deep blind mineralization by Fourier transform of a geochemical dataset. *Periodico di Mineralogia*, 90 (1).

[28]. Behera, S. and Panigrahi, M.K. (2021). Mineral prospectivity modelling using singularity mapping and multifractal analysis of stream sediment geochemical data from the auriferous Hutti-Maski schist belt, S. India. *Ore Geology Reviews*, 131, 104029.

[29]. Seyedrahimi-Niaraq, M. and Mahdiyfar, H. (2021). Introducing a new approach of geochemical anomaly intensity index (GAI) for increasing the probability of exploration of shear zone gold mineralization. *Geochemistry*. 81 (4): 125830.

[30]. Alsop, E.B., Boyd, E.S., and Raymond, J. (2014). Merging metagenomics and geochemistry reveals environmental controls on biological diversity and evolution. *BMC ecology*. 14 (1): 1-12.

[31]. Reid, M.K. and Spencer, K.L. (2009). Use of principal components analysis (PCA) on estuarine sediment datasets: the effect of data pre-treatment. *Environmental pollution*. 157 (8-9): 2275-2281.

[32]. Zuo R. (2011). Identifying geochemical anomalies associated with Cu and Pb-Zn skarn mineralization using principal component analysis and spectrum-area fractal modeling in the Gangdese Belt, Tibet (China). *Journal of Geochemical Exploration*. 1;111 (1-2): 13-22.

[33]. Heidari, S.M., Ghaderi, M., and Afzal, P. (2013). Delineating mineralized phases based on lithochemical data using multifractal model in Touzlar epithermal Au-Ag (Cu) deposit, NW Iran. *Applied Geochemistry*, 31, pp.119-132.

[34]. Yousefi, M. and Carranza, E.J.M. (2015). Prediction-area (P-A) plot and C-A fractal analysis to classify and evaluate evidential maps for mineral prospectivity modeling. *Computers & Geosciences*, 79: 69-81.

[35]. Geranian, H., Mokhtari, A.R., and Cohen, D.R. (2013). A comparison of fractal methods and probability plots in identifying and mapping soil metal contamination near an active mining area, Iran. *Science of the total environment*, 463, 845-854.

[36]. Seyedrahimi-Niaraq, M. and Mahdiyfar, H. (2022). Improvement of geochemical prospectivity mapping using power spectrum-area fractal modeling of multi-element mineralization factor (SAF-MF). *Geochemistry: Exploration, Environment, Analysis*, geochem2022-015.

[37]. Mahdiyfar H. (2019). Detection of Mo geochemical anomaly in depth using a new scenario based on spectrum-area fractal analysis. *Journal of Mining and Environment*. 1; 10 (3): 695-704.

- [38]. Zuo, R. and Wang, J. (2016). Fractal/multifractal modeling of geochemical data: A review. *Journal of Geochemical Exploration*, 164, 33-41.
- [39]. Cheng, Q. (1999). Spatial and scaling modelling for geochemical anomaly separation. *Journal of Geochemical exploration*. 65 (3): 175-194.
- [40]. Mokhtari, A.R, Rodsari P.R, Cohen, D.R, Emami A, Bafghi, A.A., and Ghegeni, Z.K. (2015). Metal speciation in agricultural soils adjacent to the Irankuh Pb–Zn mining area, central Iran. *Journal of African Earth Sciences*. 1; 101:186-93.
- [41]. Ahankoub M, Asahara Y, and Tsuboi M. (2020). Petrology and geochemistry of the Lattan Mountain magmatic rocks in the Sanandaj–Sirjan Zone, west of Iran. *Arabian Journal of Geosciences*. 13 (16): 1-3.
- [42]. Ghazban, F., McNutt, R.H., and Schwarcz, H.P. (1994). Genesis of sediment-hosted Zn-Pb-Ba deposits in the Irankuh district, Esfahan area, west-central Iran. *Economic Geology*, 89(6), pp.1262-1278.
- [43]. Fathianpour, N., Ghaedrahmati, R., and Hazery, M. (2009). Discrimination of Parts Bearing High Potential of Pb-Zn at Irankuh Region in Isfahan in GIS Environment. *Iranian Journal of Mining Engineering*, 4 (8): pp.13-22.
- [44]. Karimpour, M.H. and Sadeghi, M. (2018). Dehydration of hot oceanic slab at depth 30–50 km: KEY to formation of Irankuh-Emarat PbZn MVT belt, Central Iran. *Journal of Geochemical Exploration*, 194: 88–103.
- [45]. Hosseini-Dinani H, Aftabi A, Esmacili A, and Rabbani M. (2015). Composite soil-geochemical halos delineating carbonate-hosted zinc–lead–barium mineralization in the Irankuh district, Isfahan, west-central Iran. *Journal of Geochemical Exploration*. 1; 156:114-30.
- [46]. Ghazifard, A. and Sharief, M. (2003). The study of the extent of heavy metal absorption by agricultural crops and investigating its environmental contamination around Irankuh Pb and Zn deposit. *Isfahan Univ Res J*. 17:153–66. (in Persian).
- [47]. Kaiser, H.F. (1958). The varimax criterion for analytic rotation in factor analysis. *Psychometrika* 23, 187–200.
- [48]. Acal, C., Aguilera, A.M., and Escabias, M. (2020). New modeling approaches based on varimax rotation of functional principal components. *Mathematics*. 8 (11): p. 2085.
- [49]. Zeng, M. (2021). Estimating Latent Factor Models in Matrices and Tensors via Spectral Methods and the Varimax Rotation. The University of Wisconsin-Madison.
- [50]. Madani, N. and Sadeghi, B. (2019). Capturing Hidden Geochemical Anomalies in Scarce Data by Fractal Analysis and Stochastic Modeling. *Natural Resources Research*, 28: 833-847.
- [51]. Dobrin, M.B. and Savit, C.H. (1988). *Geophysical prospecting*: McGraw-Hill Book Co., New York, pp 867.
- [52]. Bowen, H.J.M. (1979). *The environmental chemistry of the elements*. Academic Press, London, New York.
- [53]. Zuo, R., Cheng, Q., and Xia, Q. (2009). Application of fractal models to characterization of vertical distribution of geochemical element concentration. *Journal of Geochemical Exploration*, 102: 37-43.
- [54]. Pourgholam, M.M., Afzal, P., Yasrebi, A.B., Gholinejad, M., and Wetherelt, A. (2021). Detection of geochemical anomalies using a fractal-wavelet model in Ipack area, Central Iran. *Journal of Geochemical Exploration*.220:106675.
- [55]. Mahdiyanfar, H. (2021). Identification of Buried Metal Ore Deposits using Geochemical Anomaly Filtering and Principal Factors of Power Spectrum. *Journal of Mining and Environment*. 12 (1): 205-218.

## تلفیق مدل‌های فرکتالی و مؤلفه اصلی چندمتغیره در جداسازی مناطق آلوده معدنی سرب و روی

حسین مهدیانفر<sup>1</sup>، و میرمهدی سیدرحیمی نیارق<sup>2\*</sup>

1. استادیار گروه مهندسی معدن، مجتمع آموزش عالی گناباد

2. دانشیار گروه مهندسی معدن، دانشکده فنی و مهندسی، دانشگاه محقق اردبیلی

ارسال 2023/06/06، پذیرش

\* نویسنده مسئول مکاتبات: m.seydrahimi@uma.ac.ir

## چکیده:

هدف اصلی این تحقیق، به نقشه درآوردن مناطق آلوده اطراف معدن سرب و روی ایرانکوه واقع در مرکز ایران با استفاده از تلفیق مدل تحلیل مؤلفه‌های اصلی (PCA) با مدل‌های فرکتالی عیار-غلظت (C-A) و طیف توان-مساحت (S-A) است. PCA تعداد 45 عنصر را به هشت مولفه اصلی کاهش بعد داد. مؤلفه 2، حاوی عناصر سمی سرب، روی، منگنز، کادمیوم، و باریوم، به عنوان فاکتور آلودگی شناسایی شد. این فاکتور آلودگی چندمتغیره با استفاده از روش‌های فرکتال C-A و S-A (در حوزه‌های مکانی و فرکانسی) برای ترسیم مناطق آلودگی مدل‌سازی شد. مدل‌سازی داده‌های PCA با استفاده از روش فرکتال C-A چهار جامعه اصلی را برای فاکتور آلودگی نشان داد. دو جامعه با ابعاد فرکتالی بالاتر به آلودگی ناشی از فعالیت‌های معدنی یا اثرات انسانی مرتبط هستند. ابعاد فرکتال پایین مناطق زمینه را نشان می‌دهد که تحت تأثیر این فعالیت‌ها قرار نگرفته یا کمتر تحت تأثیر قرار گرفته است. پنج جامعه ژئوشیمیایی برای فاکتور آلودگی با استفاده از مدل‌سازی فرکتالی S-A داده‌های PCA در حوزه فرکانس به دست آمد. در ادامه، جوامع مختلف ژئوشیمیایی حاصل از مدل فرکتالی در حوزه فرکانس با استفاده از فیلتر ژئوشیمیایی و تبدیل فوریه معکوس دو بعدی به دست آمدند. جوامع ژئوشیمیایی مربوط به کلاس‌های 2، 3 و 4 حاوی سیگنال‌های فرکانس متوسط، ناهنجاری آلودگی را نشان دادند. توزیع فضایی سیگنال‌های ژئوشیمیایی آلاینده، مطابقت بسیار خوبی با محدوده عملیات معدنی و محل سدباطله به عنوان منابع آلاینده نشان می‌دهد. نتایج نشان می‌دهد که غلظت عناصر سرب، روی، کادمیوم و آرسنیک در خاک‌های اطراف در مقایسه با غلظت آن‌ها در پوسته زمین، قابل توجه است. همچنین نتایج حاکی از آن است که مدل فرکتالی S-A می‌تواند با دقت بیشتری آنومالی‌های زیست‌محیطی را نسبت به مدل فرکتالی C-A، به‌ویژه در جوامع فرکانس متوسط جداسازی کند.

**کلمات کلیدی:** مدل فرکتالی، تحلیل مؤلفه اصلی، آلودگی زیست‌محیطی، سیگنال‌های ژئوشیمیایی.